International Journal of Modern Physics C
Vol. 24, No. 8 (2013) 1350052 (7 pages)

DOI: 10.1142/S0129183113500526

World Scientific
www.worldscientific.com

ELECTRONIC AND OPTICAL PROPERTIES OF PERFECT MgO AND MgO WITH *F* CENTER UNDER HIGH PRESSURE

J. ZHANG*,‡ and Z. ZENG*,†,§

*Key Laboratory of Materials Physics
Institute of Solid State Physics
Chinese Academy of Sciences
Hefei 230031, P. R. China

†Department of Physics, University
of Science and Technology of China
Hefei 230026, P. R. China
‡jzhang@theory.issp.ac.cn
§zzeng@theory.issp.ac.cn

Received 24 January 2013
Accepted 23 April 2013
Published 31 May 2013

A first-principle method is used to investigate the electronic structure and optical properties of MgO and MgO containing an oxygen vacancy. In the presence of the oxygen vacancy, a new electronic state appears in the band gap, which leads to additional peaks in the optical spectra. Furthermore, under applied pressure, the band gaps become larger, and the curves of optical properties including the dielectric function $\varepsilon(\omega)$ and absorption coefficient $\alpha(\omega)$ shift towards higher energy. The knowledge of MgO and MgO with *F* center under high pressure may provide insight into their practical applications.

Keywords: Oxygen vacancy; high pressure property; electronic and optical properties; first-principles simulation.

PACS Nos.: 71.55.Gs, 78.55.Et, 61.72.Bb, 62.50.-p.

1. Introduction

Group-II oxides have received a large interest because of their applications including catalysis, microelectronics, electronics and optoelectronics. As an important material of the Earth's lower mantle, at ambient conditions MgO crystallizes in the NaCl-type structure which is stable up to at least 227 GPa using synchrotron X-ray diffraction,[1] and the high pressure behavior of MgO has been studied theoretically.[2,3] Moreover, using density functional theory (DFT) within the generalized gradient approximation (GGA), the electronic and optical properties of MgO have been investigated

either at ambient pressure[4] or at high pressure.[5] However, during the synthesis of crystal, the intrinsic defects are easily formed in these oxides. For MgO, the main intrinsic defect is oxygen vacancy (F or color center), which will introduce defect energy levels into the forbidden gap and result in novel optical properties. Neutral F center means that the oxygen vacancy traps two electrons, which has been widely studied. Experimentally, the F center optical absorption band at 5.03 eV is observed.[6] In order to understand optical spectra, the properties of F center in MgO have been investigated with theoretical methods.[7–15] The energetics and electronic structures of a series of defects (F, F^+, F^{2+}, V, V^-, V^{2-}, and P centers) in MgO have been computed using the stationary total-energy functional.[10] The optical absorption energy of F center in MgO has been predicted by means of explicitly correlated *ab initio* cluster model calculations.[14] Recently, the calculated optical spectra based on many-body perturbation theory are in good agreement with experimental spectra, which leads to a reinterpretation of the F center's optical properties.[15] Up to now, most of the researches are devoted to the properties of MgO and MgO with F center at ambient conditions. Pressure is certainly a critical parameter for electronic and optical properties of materials, and the properties of materials at high pressure may be very different from those under normal conditions. Thus, it is significantly necessary for fundamental physics and potential applications to study the influence of pressure on the electronic and optical properties of MgO and MgO with F center.

In this paper, we present the results of DFT calculations of both perfect MgO crystal and MgO crystal containing F center. The aim is to understand the optical spectra of perfect MgO and MgO with F center under high pressure. The outline of this paper is as follows: a brief description of the initial models and the calculation methods is given in Sec. 2. In Sec. 3.1, the structural and electronic properties of MgO and MgO with F center have been presented. The optical properties through the study of the imaginary part of the dielectric function, the real part of the dielectric function and the absorption spectra are discussed in Sec. 3.2. A brief summary is given in Sec. 4.

2. Models and Methods

First-principles calculations are carried out using the projector augmented wave (PAW) method,[16] as implemented in the VASP code.[17] There are a large number of simulations on electronic structures and optical propertites of crystals using the VASP code.[4,15] For the relaxation of ions and total energy calculations, the Perdew–Burke–Ernzerhof (PBE) exchange-correlation functional is employed.[18] The cut-off energy of the plane wave basis set is chosen to be 520 eV, and a tolerance of 1.0×10^{-6} eV is adopted for the self-consistent field calculations. Forces on atoms and stress tensors are converged to within 0.001 eV/Å and 0.01 GPa, respectively. The perfect MgO crystal is calculated using the primitive cell. Oxygen vacancy calculations are made using a cubic supercell which is constructed by a $2 \times 2 \times 2$

conventional unit cell. Taking the defect site (oxygen vacancy) to be located at the origin, the unit cell contains 32 magnesium atoms and 31 oxygen atoms ($Mg_{32}O_{31}$).

Based on the relaxed structures, the electronic structure, the dielectric function, and optical absorption spectra are calculated. The dielectric function $\varepsilon(\omega) = \varepsilon_1(\omega) + i\varepsilon_2(\omega)$ is known to describe the optical response of the material. The imaginary part $\varepsilon_2(\omega)$ can be obtained after the electronic ground state has been determined. Then, from the imaginary part of the dielectric function one can also calculate the real part $\varepsilon_1(\omega)$ using the appropriate Kramers−Kronig relationship. Arising from $\varepsilon_1(\omega)$ and $\varepsilon_2(\omega)$, the other optical properties, such as the refractive index $n(\omega)$, the extinction coefficient $\kappa(\omega)$ and the absorption coefficient $\alpha(\omega)$ can be evaluated.[19]

$$n(\omega) = \left[\sqrt{\varepsilon_1^2(\omega) + \varepsilon_2^2(\omega)} + \varepsilon_1(\omega)\right]^{1/2} \Big/ \sqrt{2}, \tag{1}$$

$$\kappa(\omega) = \left[\sqrt{\varepsilon_1^2(\omega) + \varepsilon_2^2(\omega)} - \varepsilon_1(\omega)\right]^{1/2} \Big/ \sqrt{2}, \tag{2}$$

$$\alpha(\omega) = \frac{2\omega\kappa(\omega)}{c}. \tag{3}$$

3. Results and Discussions

3.1. *Structural and electronic properties*

The perfect MgO is an ionic crystal with space group $Fm\bar{3}m$ at ambient conditions. The calculated lattice parameter a is 4.239 Å which shows good agreement with the experimental result of Speziale *et al.*[20] The equilibrium lattice parameter for $Mg_{32}O_{31}$ is $a = 8.495$ Å which is bigger than that for perfect $Mg_{32}O_{32}$. In the case of the optimized $Mg_{32}O_{31}$, the existence of color center induces distortion of local geometry around the oxygen vacancy (V_o). As can be seen from Table 1, both the first-nearest neighboring (1NN) Mg atoms and the second-nearest neighboring (2NN) O atoms move slightly away from the F center at ambient pressure. With pressure increasing up to 100 GPa, the 1NN Mg atoms and the 2NN O atoms move slightly towards the F center.

Table 1. Relaxed structures for MgO with F center at different pressures. Lattice parameters and distances from the defect (V_o) position to neighboring atoms are listed.

		Distance (Å)	
Pressure (GPa)	Lattice parameters a (Å)	Mg (1NN)-V_o[a]	O (2NN)-V_o[a]
0	8.495	2.140 (0.016)	3.011 (0.007)
100	7.585	1.853 (−0.043)	2.678 (−0.004)

[a]Positive (negative) numbers in parentheses represent outward (inward) displacements with respect to the MgO lattice positions.

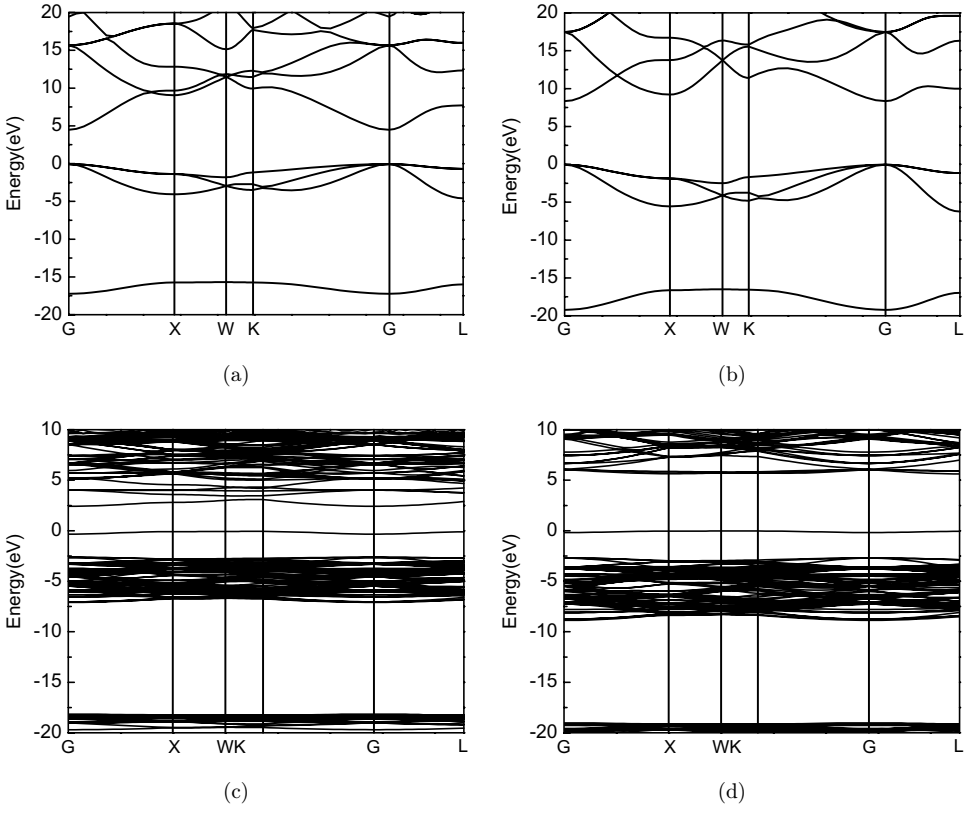

Fig. 1. Band structures: (a) perfect MgO at 0 GPa, (b) perfect MgO at 100 GPa, (c) $Mg_{32}O_{31}$ at 0 GPa and (d) $Mg_{32}O_{31}$ at 100 GPa. The top of valence band is set to be the zero energy.

For perfect MgO and MgO with F center, the band structures are shown in Fig. 1. At 0 GPa, the calculated band gap of perfect MgO is 4.5 eV which is smaller than the experimental result of 7.78 eV.[21] It is well known that DFT calculations within GGA underestimate the band gap. The perfect MgO is an insulator with a direct band gap at the brillouin zone center. For perfect MgO, the fundamental band gap increases (4.5 eV at 0 GPa and 8.4 eV at 100 GPa) with pressure increasing up to 100 GPa and the upper valence bands broaden under compression. The major difference between the band structure of perfect MgO and that of MgO containing F center is that a new energy level occurs in the forbidden band due to the oxygen vacancy.

3.2. *Dielectric functions and optical absorption spectra*

Since MgO has cubic symmetry, we need to calculate only one dielectric tensor component to completely characterize the linear optical properties. The $\varepsilon_1(\omega)$ and $\varepsilon_2(\omega)$ as functions of the photon energy are shown in Fig. 2. The dielectric function curves shift towards high energy with pressure increasing for perfect MgO and MgO

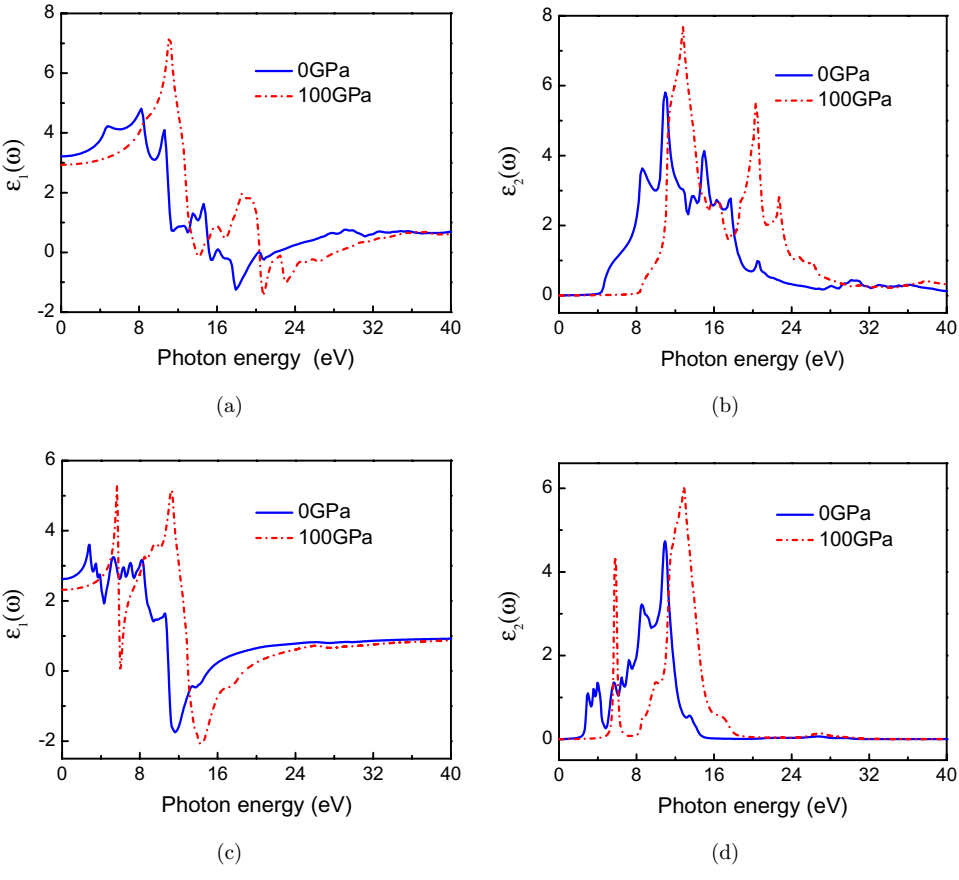

Fig. 2. (Color online) The real part $\varepsilon_1(\omega)$ and the imaginary part $\varepsilon_2(\omega)$ of dielectric function for perfect MgO and $Mg_{32}O_{31}$. (a) $\varepsilon_1(\omega)$ for MgO at 0 and 100 GPa, (b) $\varepsilon_2(\omega)$ for MgO at 0 and 100 GPa, (c) $\varepsilon_1(\omega)$ for $Mg_{32}O_{31}$ at 0 and 100 GPa and (d) $\varepsilon_2(\omega)$ for $Mg_{32}O_{31}$ at 0 and 100 GPa.

containing F center. In a high-energy area (>32 eV), the value of the real part changes very little, while that of the imaginary part is very small. At ambient conditions, our calculated results show good agreement with the previously reported theoretical investigations for perfect MgO.[4] In the real part, the calculated static dielectric constant $\varepsilon_1(0)$ is 3.22 at 0 GPa and 2.93 at 100 GPa for MgO. When the oxygen vacancy is introduced, $\varepsilon_1(0)$ is 2.62 at 0 GPa and 2.32 at 100 GPa, which indicates that the oxygen vacancy reduces $\varepsilon_1(0)$. Additionally, as the pressure is increased from 0 GPa to 100 GPa, the static dielectric constant $\varepsilon_1(0)$ decreases for perfect MgO and MgO with F center. The imaginary part of the dielectric function is directly related to the band structure of a solid. In the imaginary part, $\varepsilon_2(\omega)$ curves have thresholds of transition close to the band gap values of the corresponding compounds. The peaks in $\varepsilon_2(\omega)$ curves originate from the electron transitions between the occupied and unoccupied states. For the perfect MgO at 0 GPa, the peaks

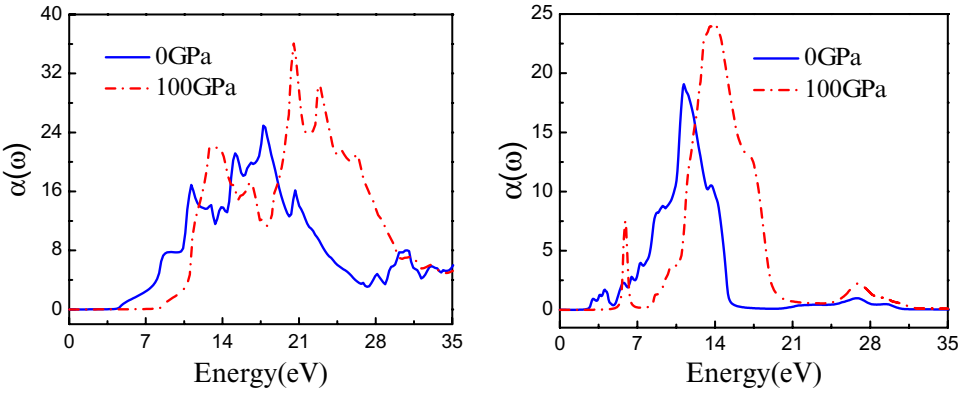

Fig. 3. (Color online) Absorption spectra $\alpha(\omega)$: (a) perfect MgO at 0 and 100 GPa and (b) $Mg_{32}O_{31}$ at 0 and 100 GPa.

centered at 11.0, 13.9, 16.3, 17.7 and 20.5, agree with experimental observation of 10.8, 13.3, 16.8, 17.3 and 20.5 eV.[22] The peaks localized at around 8.6 and 11.0 eV, are mainly due to direct transitions between the upper valence band and the first conduction band above Fermi energy level at L-point and K-point, respectively. At 100 GPa, the main peak positioned at 12.8 eV arises from direct transitions at K-point. The highest peak in imaginary part increases with pressure increasing. The $\varepsilon_2(\omega)$ curve of $Mg_{32}O_{31}$ has additional peaks below 4.5 eV (0 GPa) and 8.4 eV (100 GPa) due to the oxygen vacancy compared with the $\varepsilon_2(\omega)$ curve of perfect MgO.

The absorption spectra $\alpha(\omega)$ of the perfect MgO under 0 and 100 GPa, and $Mg_{32}O_{31}$ under 0 and 100 GPa are given in Figs. 3(a) and 3(b), respectively. For $Mg_{32}O_{31}$ at ambient pressure, although the peak centered at 3.5 eV is associated with the oxygen vacancy, the value of the peak is underestimated by 1.5 eV compared with experimentally observed F center absorption energy of 5.03 eV.[6] The main reason for discrepancy is the underestimation of the band gap. Additionally, the positions of the main peaks are shifted towards higher energy under pressure while they still have the same type as those at zero pressure.

4. Conclusion

The electronic structures and optical properties for pure MgO and MgO with an oxygen vacancy ($Mg_{32}O_{31}$) have been studied using the pseudopotential plane wave method. The introduced oxygen vacancy leads to the distortion of local geometry. The line shapes of the dielectric function and adsorption coefficient are almost unchanged while there is a little shift forward high-energy region, when perfect MgO and $Mg_{32}O_{31}$ are compressed to 100 GPa. Meanwhile, the MgO with oxygen vacancy exhibits additional absorption peaks compared with that of pure MgO at the same pressure.

Acknowledgments

This work was supported by the National Science Foundation of China under Grants Nos. 11174284 and NSAF U1230202, the special Funds for Major State Basic Research Project of China (973) under Grant No. 2012CB933702, and Director Grants of CASHIPS. The calculations were performed in Center for Computational Science of CASHIPS and on the ScGrid of Supercomputing Center, Computer Network Information Center of Chinese Academy of Sciences.

References

1. T. S. Duffy, R. J. Hemley and H.-K. Mao, *Phys. Rev. Lett.* **74**, 1371 (1995).
2. J. E. Jaffe, J. A. Snyder, Z. Lin and A. C. Hess, *Phys. Rev. B* **62**, 1660 (2000).
3. A. R. Oganov and P. I. Dorogokupets, *Phys. Rev. B* **67**, 224110 (2003).
4. A. Schleife, F. Fuchs, J. Furthmüller and F. Bechstedt, *Phys. Rev. B* **73**, 245212 (2006).
5. Z.-J. Liu, Y.-X. Du, X.-L. Zhang, J.-H. Qi, L.-N. Tian and Y. Guo, *Phys. Status Solidi B* **247**, 157 (2010).
6. L. A. Kappers, R. L. Kroes and E. B. Hensley, *Phys. Rev. B* **1**, 4151 (1970).
7. B. M. Klein, W. E. Pickett, L. L. Boyer and R. Zeller, *Phys. Rev. B* **35**, 5802 (1987).
8. R. Pandey and J. M. Vail, *J. Phys. Condens. Matter.* **1**, 2801 (1989).
9. A. D. Vita, M. J. Gillan, J. S. Lin, M. C. Payne, I. Štich and L. J. Clarke, *Phys. Rev. B* **46**, 12964 (1992).
10. A. Gibson, R. Haydock and J. P. Lafemina, *Phys. Rev. B* **50**, 2582 (1994).
11. E. Scorza, U. Birkenheuer and C. Pisani, *J. Chem. Phys.* **107**, 9645 (1997).
12. F. Illas and G. Pacchioni, *J. Chem. Phys.* **108**, 7835 (1998).
13. C. Jun, L. Lin, T. Lu and L. Yong, *Eur. Phys. J. B* **9**, 593 (1999).
14. C. Sousa and F. Illas, *J. Chem. Phys.* **115**, 1435 (2001).
15. P. Rinke, A. Schleife, E. Kioupakis, A. Janotti, C. Rödl, F. Bechstedt, M. Scheffler and C. G. V. de Walle, *Phys. Rev. Lett.* **108**, 126404 (2012).
16. G. Kresse and D. Joubert, *Phys. Rev. B* **59**, 1758 (1999).
17. G. Kresse and J. Furthmüller, *Phys. Rev. B* **54**, 11169 (1996).
18. J. P. Perdew, K. Burke and M. Ernzerhof, *Phys. Rev. Lett.* **77**, 3865 (1996).
19. P. Y. Yu and M. Cardona, *Fundamentals of Semiconductors*, 4th edn. (Springer-Verlag, Berlin, 2010).
20. S. Speziale, C.-S. Zha, T. S. Duffy, R. J. Hemley and H.-K. Mao, *J. Geophys. Res.* **106**, 515 (2001).
21. R. C. Whited and W. C. Walker, *Phys. Rev. Lett.* **22**, 1428 (1969).
22. D. M. Roessler and W. C. Walker, *Phys. Rev.* **159**, 733 (1967).